Oncogene (2010) 29, 2228–2237

www.nature.com/onc

ORIGINAL ARTICLE

Accelerated hepatocellular carcinoma development in mice expressing the *Pim-3* transgene selectively in the liver

Y Wu[1,2], YY Wang[2], Y Nakamoto[3], Y-Y Li[2,4], T Baba[2], S Kaneko[3], C Fujii[2,5] and N Mukaida[2]

[1]*Department of Hematology and Hematology research Laboratory, State Key Laboratory of Biotherapy and Cancer Center, West China Hospital, Sichuan University, Chengdu, Sichuan Province, PR China;* [2]*Division of Molecular Bioregulation, Cancer Research Institute, Kanazawa University, 13-1 Takara-machi, Kanazawa, Japan;* [3]*Department of Disease Control and Homeostasis, Graduate School of Medical Sciences, Kanazawa University, 13-1 Takara-machi, Kanazawa, Japan and* [4]*Researcher Center, Fudan University Cancer Hospital, Shanghai, PR China*

Pim-3, a proto-oncogene with serine/threonine kinase activity, was enhanced in hepatocellular carcinoma (HCC) tissues. To address the roles of Pim-3 in HCC development, we prepared transgenic mice that express human Pim-3 selectively in liver. The mice were born at a Mendelian ratio, were fertile and did not exhibit any apparent pathological changes in the liver until 1 year after birth. Pim-3-transgenic mouse-derived hepatocytes exhibited accelerated cell cycle progression. The administration of a potent hepatocarcinogen, diethylnitrosamine (DEN), induced accelerated proliferation of liver cells in Pim-3 transgenic mice in the early phase, compared with that observed for wild-type mice. Treatment with DEN induced lipid droplet accumulation with increased proliferating cell numbers 6 months after the treatment. Eventually, wild-type mice developed HCC with a frequency of 40% until 10 month after the treatment. Lipid accumulation was accelerated in Pim-3 transgenic mice with higher proliferating cell numbers, compared with that observed for wild-type mice. Pim-3 transgenic mice developed HCC with a higher incidence (80%) and a heavier burden, together with enhanced intratumoral CD31-positive vascular areas, compared with that observed for wild-type mice. These observations indicate that Pim-3 alone cannot cause, but can accelerate HCC development when induced by a hepatocarcinogen, such as DEN.
Oncogene (2010) **29,** 2228–2237; doi:10.1038/onc.2009.504; published online 18 January 2010

Keywords: serine/threonine kinase; apoptosis; cell cycle; Bad

Correspondence: Dr N Mukaida, Division of Molecular Bioregulation, Cancer Research Institute, Kanazawa University, 13-1 Takara-machi, Kanazawa, Ishikawa 920-0934, Japan.
E-mail: naofumim@kenroku.kanazawa-u.ac.jp
[5]Present address, Department of Integrative Physiology, School of Medicine, Shinshu University, 3-1-1 Asahi, Matsumoto 390-8621, Japan.
Received 13 May 2009; revised 25 October 2009; accepted 7 December 2009; published online 18 January 2010

Introduction

There were over 667 000 new cases of hepatocellular carcinoma (HCC) worldwide in 2005. The 5-year survival rate of individuals with hepatic malignancy is only 8.9% despite aggressive conventional therapy, making hepatic malignancy the second most lethal cancer among human malignancies (Farazi and DePinho, 2006; Umemura *et al.*, 2009). Hepatocellular carcinoma usually arises in conditions that can cause liver cirrhosis, such as chronic hepatitis B and C viral infection, chronic alcohol consumption and intake of food contaminated with aflatoxin-B_1 (Zheng *et al.*, 2007). These conditions generally provoke continuous rounds of hepatocyte damage in the setting of chronic hepatitis or liver cirrhosis, and eventually activate resident or inflammatory non-parenchymal cells to produce growth factors and cytokines (Otani *et al.*, 2005). The produced factors can drive compensatory and aberrant proliferation of surviving hepatocytes and development of pre-malignant dysplastic nodules that form the nucleus of neoplastic lesions. Only recently has the molecular analysis of human HCC unraveled many genetic and epigenetic alterations that result in the deregulation of key proto-oncogenes and tumor-suppressor genes, including TP53, β-catenin, ErbB receptors family members, *met* and its ligand, hepatocyte growth factor, p16, E-cadherin and cyclo-oxygenase 2 (Hosono *et al.*, 1993). However, roles of other proto-oncogenes and tumor suppressor genes in HCC development still remain elusive (Thorgeirsson and Grisham, 2002).

We previously identified *Pim-3*, a proto-oncogene with serine/threonine kinase activity, as the gene selectively expressed in pre-malignant and malignant lesions of the mouse HCC model in transgenic mice expressing hepatitis B virus surface antigen (Fujii *et al.*, 2005). *Pim-3* was originally identified as a depolarization-induced gene, *KID-1*, in PC12 cells, a rat pheochromocytoma cell line (Feldman *et al.*, 1998). Subsequently, Deneen *et al.* (2003) demonstrated that *Pim-3* gene transcription was enhanced in the EWS/ETS-induced malignant transformation of NIH 3T3 cells, suggesting the involvement of Pim-3 in tumorigenesis. Consistently, we observed that Pim-3 expression was enhanced in

carcinomas but not in normal tissues of human endoderm-derived organs, including the liver (Fujii *et al.*, 2005), pancreas (Li *et al.*, 2006), colon (Popivanova *et al.*, 2007) and stomach (Zheng *et al.*, 2008). Moreover, Pim-3 can inactivate a pro-apoptotic molecule, Bad, and maintain the expression of an anti-apoptotic molecule, Bcl-X_L, and prevent apoptosis of human pancreatic cancer and colon cancer cells (Li *et al.*, 2006). Similarly, the ablation of endogenous Pim-3 by short interfering RNA reduced the cell growth of human HCC cell lines by inducing their apoptosis (Fujii *et al.*, 2005).

These observations prompted us to investigate the effects of liver-specific Pim-3 overexpression on HCC development. Although we could not observe spontaneous HCC development in liver-specific Pim-3 transgenic mice, these mice developed HCC with a higher incidence and a heavier hepatocarcinoma burden, when a potent hepatocarcinogen, diethylnitrosamine (DEN), was administered during the suckling period. These results suggest that Pim-3 can accelerate but is not likely the primary inducer of HCC development.

Results

Characterization of transgenic mice overexpressing Pim-3 under the control of the albumin promoter

Pim-3 transgenic mice were born at a Mendelian ratio, were fertile and did not show any apparent abnormalities in the liver until 1 year after birth (data not shown). We first examined the expression pattern of Pim-3 in Pim-3 transgenic mice. Mouse *Pim-3* messenger RNA (mRNA) was detected in liver at a similar extent in both wild-type (WT) and Pim-3 transgenic mice, whereas human *Pim-3* mRNA was exclusively detected in Pim-3 transgenic mice (Figure 1b). Consistently, Pim-3 protein was detected abundantly in liver of Pim-3 transgenic mice but not WT mice (Figure 1b). Pim-3 protein was also detected in the heart and kidney of Pim-3 transgenic mice, but not of WT mice (Figure 1c). As anti-Pim-3 recognizes both human and mouse Pim-3 to a similar degree, we further examined the mRNA of human and mouse Pim-3 in the liver, heart and kidney. Human *Pim-3* mRNA was detected in the liver of Pim-3 transgenic mice, but not in other organs (Figure 1d). These observations would indicate that Pim-3 transgenic mice express human Pim-3 abundantly and selectively in liver.

Enhanced hepatocyte proliferation by Pim-3 overexpression

As Pim-3 can phosphorylate a pro-apoptotic molecule, Bad, at the Ser^{112} residue but not at the Ser^{136} residue, we first examined the phosphorylation states of Bad, to prove the functionality of the *Pim-3* gene, selectively overexpressed in liver. Bad was constitutively phosphorylated at Ser^{112} in hepatocytes from Pim-3 transgenic but not WT mice (Figure 2a). However, the level of phospho-Ser^{136}–Bad was not enhanced in Pim-3 transgenic mice. These observations would indicate that overexpressed Pim-3 was functional in terms of its capacity to phosphorylate Bad, its substrate. The levels of cyclin D1 and proliferating cell nuclear antigen (PCNA) in hepatocytes were increased in Pim-3 transgenic mice, compared with that observed for WT mice (Figure 2b). Moreover, cell cycle analysis of isolated heptocytes revealed that the proportion of the cells in subG1 phase, which represent apoptotic cells, was marginally but not significantly decreased in Pim-3 transgenic mice. However, the proportion of the cells in G2/M phase was significantly increased in Pim-3 transgenic mice compared with that observed for WT mice (Figure 2c). To exclude the possibility that

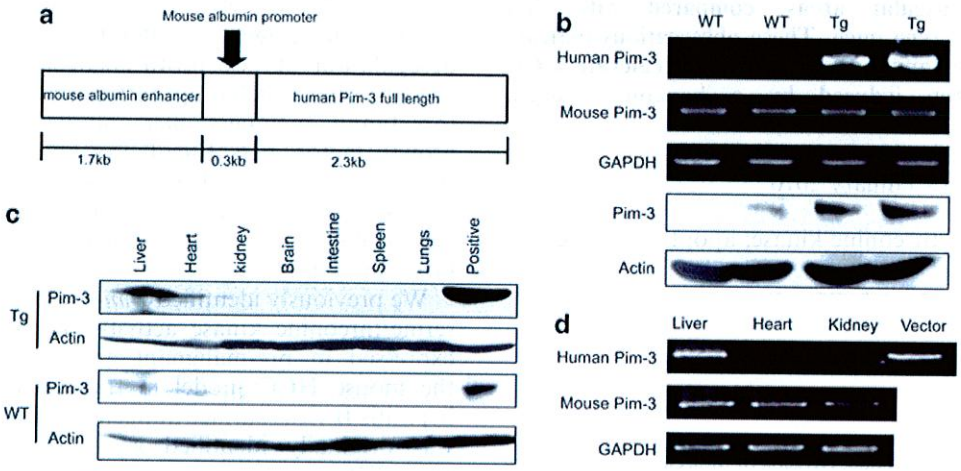

Figure 1 Expression of Pim-3 in alb-Pim-3 transgenic mice. (**a**) The schematic representation of the gene used for preparation of Pim-3 transgenic mice. (**b**) Expression of human (transgenic) and mouse (endogenous) *Pim-3* mRNA and protein levels in liver. The upper three lines are assessed by RT–PCR, whereas the lower two lines are assessed by immunoblotting. Representative results from five independent animals are shown here. (**c**) Immunoblotting analysis of Pim-3 protein expression in the liver, heart, kidney, brain, intestine, spleen and lungs of Pim-3 transgenic mice. The human embryonic kidney (HEK293) cells transfected with human Pim-3 complementary DNA (cDNA) were used as a positive control. Representative results from five independent animals are shown here. (**d**) Endogenous mouse *Pim-3* mRNA expression in the liver, heart and kidney of Pim-3 transgenic mice were determined by RT–PCR. Representative results from five independent animals are shown here.

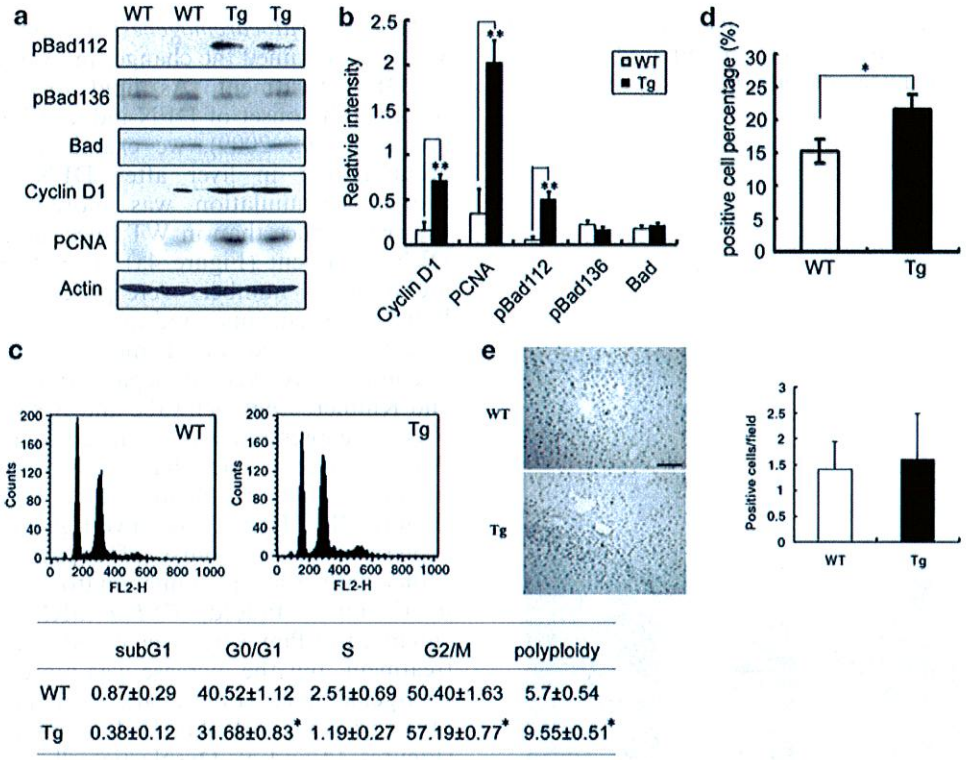

	subG1	G0/G1	S	G2/M	polyploidy
WT	0.87±0.29	40.52±1.12	2.51±0.69	50.40±1.63	5.7±0.54
Tg	0.38±0.12	31.68±0.83*	1.19±0.27	57.19±0.77*	9.55±0.51*

Figure 2 The effects of Pim-3 overexpression on hepatocyte functions. Hepatocytes were obtained from 3-week-old wild-type (WT) and Pim-3 transgenic (Tg) mice and used for the following analyses. (**a** and **b**) Protein was extracted from purified hepatocytes from WT and Tg mice, and was subjected to immunoblotting using anti-phospho-Ser^{112}-Bad, anti-phospho-Ser^{136}-Bad, anti-Bad, anti-cyclin D1 and anti-PCNA (proliferating cell nuclear antigen) antibodies as described in Materials and methods section. Representative results from four independent experiments are shown in (**a**). The intensity of each band was determined using National Institutes of Health (NIH) Image Analysis software version 1.62 (NIH, Bethesda, MD, USA), and its ratios to β-actin were calculated and are shown in (**b**) ($n=4$). Open boxes, WT mice; closed boxes, Pim-3 Tg mice. $^{**}P<0.01$. (**c**) DNA contents were determined for hepatocytes from WT and Pim-3 Tg mice as described in Materials and methods section. Representative results from five independent experiments are shown here. After the proportion of each fraction was determined, mean and 1 s.d. were calculated and are shown in the Table (inlet; $n=5$). $^{\#}P<0.05$; $^{*}P<0.01$. (**d**) The proportion of cyclin B1-positive cells was determined on liver tissues obtained from 3-week-old Pim-3 trangenic and WT mice as described in Materials and methods section. Mean and s.e.m. values were calculated ($n=6$) and are shown here. (**e**) The terminal transferase dUTP nick end labeling (TUNEL) assay was conducted as described in Materials and methods section. Representative results from five individual animals are shown in the left panel. Positive cells were determined in five randomly chosen fields (× 400) from each animal by an examiner without any knowledge of experimental procedures. Mean ± s.d. values are shown in the right panel ($n=5$).

isolation of hepatocytes from liver gave rise to artificially high proportion of cells in G2/M phase, we also enumerated the proportion of cells in G2/M phase by immunostaining liver tissues with anti-cyclin B1 antibodies. The proportion of cyclin B1-positive cells were significantly higher in Pim-3 transgenic mice than in WT mice (Figure 2d). Moreover, TUNEL (terminal transferase dUTP nick end labeling) staining failed to detect any significant differences in the numbers of apoptotic hepatocytes between untreated WT and Pim-3 transgenic mice (Figure 2e). These observations suggest that Pim-3 overexpressed in liver can accelerate the cell cycle progression of hepatocytes.

Enhanced liver damage in Pim-3 transgenic mice

We then treated Pim-3 transgenic and WT mice with DEN, a potent hepatocarcinogen. Both Pim-3 transgenic and WT mice survived exposure to DEN. Serum alanine amino transferase levels, a marker of liver injury, increased with maximal levels less than 1 000 IU/l, and were significantly but not markedly higher in Pim-3 transgenic mice than in WT mice (Figure 3a). These observations suggest that DEN-induced acute liver injury was mild. This may account for comparable levels of apoptosis in liver after DEN treatment until 72 h after the injection (Figures 3b and c). In contrast, PNCA and cyclin D1 levels were higher, at 72 h after the injection in Pim-3 transgenic mice, than those observed for WT mice (Figures 3d and e). Moreover, proliferating cells were progressively increased in the centrilobular region of Pim-3 transgenic mice and to a lesser degree in WT mice (Figures 3f and g). The crucial involvement of tumor necrosis factor (TNF)-α in hepatocyte proliferation (Yamada *et al*., 1997) prompted us to determine intrahepatic expression of TNF-α mRNA levels. The TNF-α mRNA levels were increased significantly at 48 h after DEN treatment (Figure 3h). These observations

indicate that the DEN challenge enhanced liver damage in Pim-3 transgenic mice, compared with that observed for WT mice, despite increased hepatocyte proliferation.

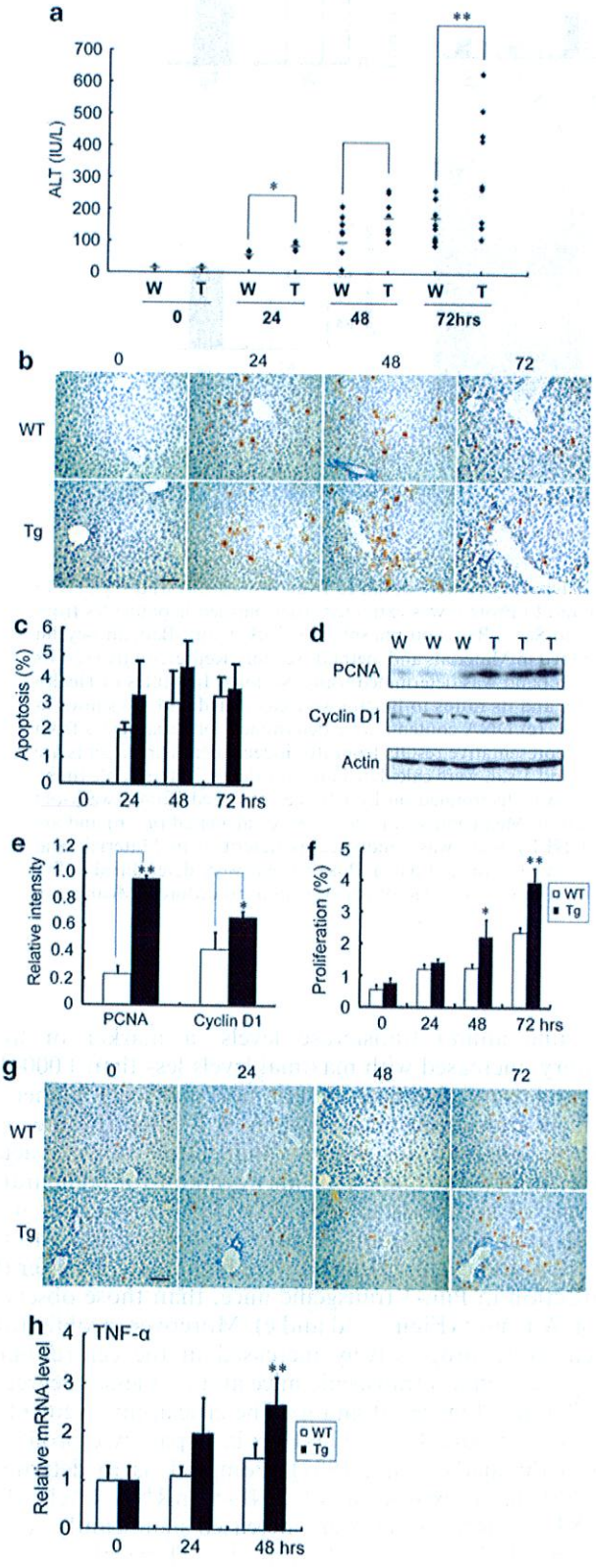

Enhanced hepatocarcinogenesis in Pim-3 transgenic mice

We next examined the changes in liver in the later phase of DEN treatment. As lipid droplet accumulation precedes the onset of DEN-induced HCC development (Wang *et al.*, 2009), we examined the lipid droplet accumulation in liver after DEN treatment. Lipid droplet accumulation was more evident in Pim-3 transgenic mice than in WT mice, until 6 months after DEN treatment (Figure 4a). The PCNA-positive proliferating cell numbers were progressively increased in Pim-3 transgenic mice and to a lesser degree in WT mice (Figures 4b and c). Tumor necrosis factor-α was potentially involved in hepatocarcinogenesis (Roberts and Kimber, 1999; Schwabe and Brenner, 2006). Moreover, its expression was enhanced to a greater extent in Pim-3 transgenic mice than that observed for WT mice promptly after treatment with a high-dose of DEN (Figure 3h). Hence, we investigated *TNF-α* mRNA expression in the course of hepatocarcinogenesis together with other pro-inflammatory cytokines, such as interleukin-1. Indeed, *TNF-α* mRNA expression was enhanced in Pim-3 transgenic and WT mice after DEN treatment, but the increase was more evident in Pim-3 transgenic mice (Figure 4f). A similar tendency was observed for interleukin-1β but not for interleukin-1α (Figures 4d and e). Dysplastic cells were observed and lobules were distorted in livers of Pim-3 transgenic mice, but not of WT mice, 6 months after DEN treatment (Figure 5a). At 10 months after the injection, nodules consisting of highly dysplastic malignant cells were observed in liver of Pim-3 transgenic mice and to a lesser extent in WT mice (Figure 5a). Macroscopically,

Figure 3 The effects of overexpressed Pim-3 on apoptosis and cell proliferation after diethylnitrosamine (DEN) treatment. (**a**) Serum alanine amino transferase (ALT) levels were determined as described in Materials and methods section. Each symbol indicates serum ALT level of each animal and the bars represent the median of each group. $*P<0.05$; $**P<0.01$ vs wild-type (WT) mice. (**b** and **c**) Liver tissues were obtained from WT or transgenic (Tg) mice at the indicated time intervals and immunostained with anti-cleaved caspase 3 antibody. Representative results from five independent animals are shown in (**b**) with an original magnification ×400. Proportion of cleaved caspase 3-positive apoptotic cells were determined as described in Materials and methods section. Mean ± s.d. values are shown in (**c**) ($n=5$). Open boxes, WT mice; closed boxes, Pim-3 transgenic mice. (**d** and **e**) Cell lysates were obtained from liver of WT (W) and Pim-3 transgenic mice (T) at 72 h after DEN treatment and subjected to immunoblotting using anti-PCNA (proliferating cell nuclear antigen) or anti-cyclin D1 antibodies. Representative results from three independent experiments are shown in (**d**). The intensity of each band was determined and its ratio to β-actin was calculated. Mean ± s.d. values are shown in (**e**) ($n=5$). Open boxes, WT mice; closed boxes, Pim-3 transgenic mice. $*P<0.05$; $**P<0.01$ vs WT mice. (**f** and **g**) Liver tissues were obtained from WT or Tg mice at the indicated time intervals and immunostained with anti-PCNA antibody. Representative results from five independent animals are shown in (**g**) with an original magnification ×400. PCNA-positive proliferating cell numbers were determined as described in Materials and methods section. Mean ± s.d. values are shown in (**f**) ($n=5$). $*P<0.05$; $**P<0.01$ vs WT mice. (**h**) Intrahepatic tumor necrosis factor-α (*TNF-α*) mRNA levels were determined as described in Materials and methods section. $**P<0.01$ vs WT mice ($n=5$).

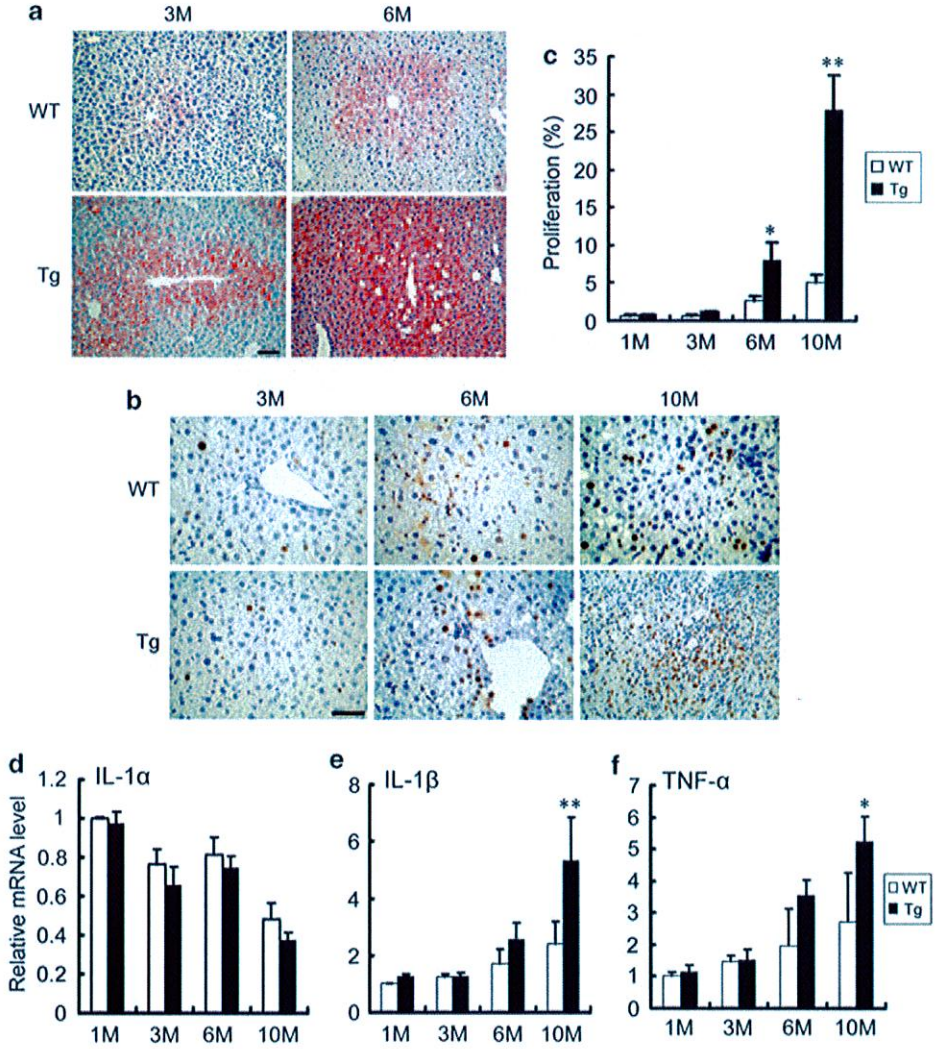

Figure 4 The effects of Pim-3 overexpression in liver pathology in the later phase after diethylnitrosamine (DEN) treatment. (**a**) The liver was obtained from wilt-type (WT) or Pim-3 transgenic mice (Tg) at the indicated time intervals and was subjected to staining with oil red solution as described in Materials and methods section. Representative results from five independent animals are shown with an original magnification ×200. (**b** and **c**) The livers were obtained from WT or Pim-3 Tg mice at the indicated time intervals and were subjected to immunostaining with anti-PCNA (proliferating cell nuclear antigen) antibody as described in Materials and methods section. Representative results from five independent animals are shown in (**b**) with an original magnification ×400. PCNA-positive cell numbers were determined as described in Materials and methods section. Mean ± s.d. values are shown in (**c**) ($n=5$). Open boxes, WT mice; closed boxes, Pim-3 Tg mice. $^{*}P<0.05$; $^{**}P<0.01$ vs WT mice.(**d**, **e** and **f**) Total RNA was extracted from the liver of WT or Pim-3 Tg mice at the indicated time intervals after DEN treatment and were subjected to a semi-quantitative RT–PCR analysis for the detection of mRNA for interleukin (IL)-1α (**d**), IL-1β (**e**), and tumor necrosis factor (TNF)-α (**f**). The ratio of each cytokine was calculated as described in Materials and methods section. Each value represents mean ± s.d. value ($n=5$). Open boxes, WT mice; closed boxes, Pim-3 Tg mice. $^{*}P<0.05$; $^{**}P<0.01$ vs WT mice.

approximately half of male WT mice developed HCC nodules at 10 months after DEN injection (Figures 5b–d), consistent with the previous report (Yang *et al.*, 2006). In contrast, most Pim-3 transgenic mice developed HCC nodules by 10 months after DEN treatment, with higher relative liver weight and larger numbers of HCC nodules than WT mice (Figures 5b–e). The enhanced hepatocarcinogenesis in Pim-3 transgenic mice may mirror the fact that neovascularization, an essential process for hepatocarcinogenesis, was augmented in Pim-3 transgenic mice compared with that observed for WT mice, as demonstrated by increases in CD31-positive areas in the liver (Figures 5f and g).

Discussion

We previously observed that Pim-3 was expressed selectively in pre-malignant and malignant lesions of the mouse HCC model in transgenic mice expressing hepatitis B virus surface antigen (Fujii *et al.*, 2005). Moreover, Pim-3 protein was detected in a substantial proportion of HCC cells and precancerous lesions in human liver samples, but not normal human liver. Furthermore, Pim-3 protein was also detected in regenerating bile ductules that are assumed to be the proliferation of hepatic stem cells after chronic injury. These observations suggested potential roles of aberrantly expressed Pim-3 in hepatocarcinogenesis. To

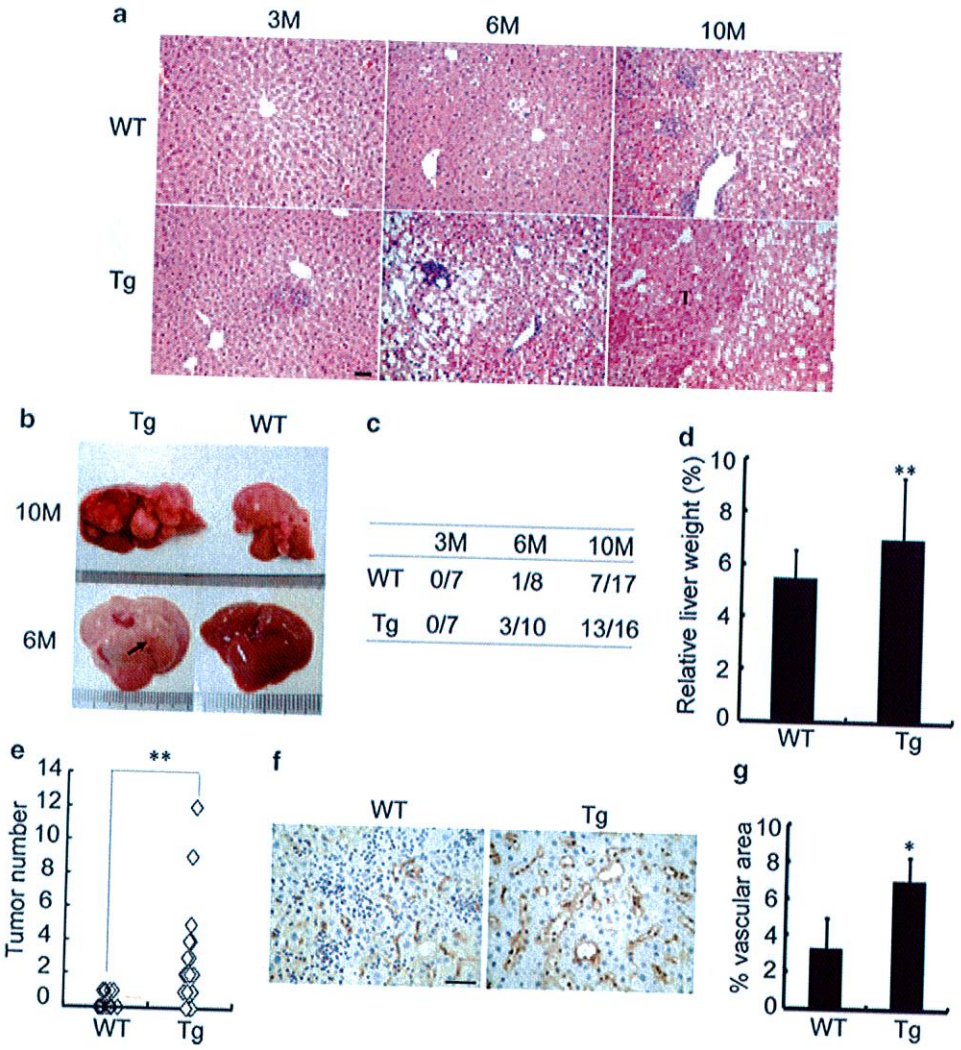

Figure 5 Enhanced hepatocarcinogenesis in Pim-3 transgenic (Tg) mice. **(a)** The liver tissues were obtained from wild-type (WT) or Pim-3 Tg mice at the indicated time intervals after DEN treatment and subjected to hematoxylin and eosin (HE) staining. Representative results from five individual animals are shown here with an original magnification ×200. **(b)** Macroscopic appearance of liver at 10 and 6 months after DEN treatment. Representative results from eight animals are shown here. Left panels: Pim-3 Tg mice; right panels: WT mice. The arrow indicates a small tumor nodule. **(c)** Incidence of macroscopic tumor formation at the indicated time intervals after DEN treatment in WT and Pim-3 Tg mice. **(d)** Liver weight relative to whole body weight was determined for WT and Pim-3 Tg mice at 10 months after DEN treatment. Each value represents mean ± s.d. value ($n=5$). $^{**}P<0.01$ vs WT mice. **(e)** Numbers of tumors with a diameter of larger than 1 mm were determined in the livers of WT ($n=17$) or Pim-3 Tg mice ($n=16$) at 10 months after DEN treatment. Each symbol indicates the tumor numbers of each animal and the bars represent the median of each group. $^{**}P<0.01$ vs WT mice. **(f** and **g)** The liver tissues were obtained from WT or Pim-3 Tg mice at 10 months after DEN treatment and were subjected to immunostaining with anti-CD31 antibody. Representative results from five individual animals are shown in **(f)** with an original magnification ×400. CD31-positive vascular areas within tumors were determined as described in Materials and methods section. Mean and s.d. values were calculated and are shown in **(g)**. $^{*}P<0.05$ vs WT mice.

address the roles of Pim-3, we generated transgenic mice that constitutively express human Pim-3 selectively in liver. Untreated hepatocytes derived from these transgenic mice exhibited enhanced cell proliferation compared with those obtained from WT mice. However, these transgenic mice did not develop HCC spontaneously. Hence, enhanced cell proliferation cannot *per se* result in carcinogenesis in liver.

Kinase activation generally requires a posttranslational modification, particularly, phosphorylation in its regulatory domain. However, another member of the Pim kinase family, Pim-1, is constitutively active without any further alteration in its conformation because it lacks any regulatory domain (Qian *et al.*, 2005). Similarly, Pim-3 lacks any regulatory domain (Fujii *et al.*, 2005) and *Pim-3* complementary DNA (cDNA) alone induced phosphorylation of its target protein, Bad, at Ser^{112} when it was transfected into human pancreatic cancer cell lines (Li *et al.*, 2006). Consistently, Pim-3 transgenic mice exhibited enhanced phosphorylation of Bad at Ser^{112} in the liver. The proapoptotic activity of Bad is regulated by its phosphorylation at

Ser[112] or Ser[136] (She *et al.*, 2005). Unphosphorylated Bad binds and eventually inactivates anti-apoptotic family members, primarily Bcl-X_L and even Bcl-2 (Yang *et al.*, 1995; Zha *et al.*, 1996). As phosphorylation of Bad at Ser[112] or Ser[136] can result in the liberation of Bcl-X_L and Bcl-2, which can prevent apoptosis (Chen *et al.*, 2005), phosphorylated Bad represents its inactive form. However, both WT and Pim-3 transgenic mice developed apoptosis in liver to a similar extent when they were treated with a potent hepatocarcinogen, DEN. These observations suggest that phosphorylated Bad is not sufficient to prevent apoptosis induced by potent hepato-cytotoxic drugs such as DEN.

Pim-3 transgenic mice developed HCC with a higher incidence and a heavier burden than WT mice when both were treated similarly with DEN. Hepatocytes, particularly those in the centrilobular region, metabolized DEN into an alkylating agent that, in turn, can induce DNA damage and mutations in hepatocytes (Verna *et al.*, 1996). Simultaneously, DEN metabolites can generate reactive oxygen species (ROS) (Kamata *et al.*, 2005; Schwabe and Brenner, 2006). When treated with DEN, mice with liver-specific deletion of an essential kinase for NF-κB activation, IKKβ, generated increased levels of ROS in hepatocytes, together with enhanced hepatocyte death and augmented compensatory hepatocyte proliferation. The net result was exaggerated HCC development with a high cell proliferation rate as evidenced by increased PCNA- and cyclin D1-positive cell numbers in liver (Maeda *et al.*, 2005). Similarly, DEN treatment augmented hepatocyte proliferation but not apoptosis in Pim-3 transgenic mice compared with that observed in WT mice, as evidenced by increased PCNA- and cyclin D1-positive cell numbers in liver. These data may account for accelerated hepatocarcinogenesis in Pim-3 transgenic mice. However, several lines of evidence indicate the potential involvement of other Pim kinases, Pim-1 and Pim-2, in NF-κB activation (Hammerman *et al.*, 2004; Zemskova *et al.*, 2008). Thus, it still remains to be investigated whether the *Pim-3* transgene can induce ROS generation in a similar manner as the IKKβ deletion.

Liver injury causes liver regeneration primarily through hepatocyte division but if hepatocyte division is impaired, liver repair requires the recruitment of hepatic oval cells (Ma *et al.*, 2006). Oval cells mainly express α-fetoprotein but not albumin, and can proliferate and differentiate into both hepatocytes and bile duct cells. Several independent groups claimed that HCC cells can arise from oval cells (Braun *et al.*, 1989). Mice deficient in the *IKKβ* gene in liver developed HCC with an incidence higher than WT mice (Maeda *et al.*, 2005). In this mouse, the *IKKβ* gene was deleted by using cre recombinase expressed under the control of an albumin promoter/enhancer and therefore, the gene was deleted selectively in albumin-expressing hepatocytes but not in oval cells. As we used the same promoter/enhancer to prepare transgenic mice, it is likely that the *Pim-3* transgene was expressed selectively in hepatocytes but not in oval cells. Thus, the *Pim-3* transgene mainly acted on hepatocytes to promote carcinogenesis, although its effects on oval cell proliferation cannot completely be excluded.

Accumulating evidence indicates that Pim-1, a member of the Pim kinase family, can progress cell cycle by phosphorylating several cell cycle regulators and altering their activities. Pim-1 can phosphorylate the phosphatase, Cdc25A, thereby increasing its phosphatase activity (Mochizuki *et al.*, 1999). Moreover, Pim-1 can phosphorylate G1-specific inhibitor p21 (Waf), a cyclin-dependent kinase inhibitor, and induce its cytoplasmic localization (Wang *et al.*, 2002). Furthermore, Pim-1 can phosphorylate the kinase Cdc25C-associated kinase (C-TAK)-1 and decrease its kinase activity (Bachmann *et al.*, 2004), whereas Pim-1 can phosphorylate and activate the G2/M-specific phosphatase Cdc25C. Alteration of the activities of these molecules can result in cell cycle progression, particularly during the G2/M phase. Pim-3 and Pim-1, but not Pim-2, bind to a consensus peptide substrate (AKRRRHPSGPPTA) with a strikingly high affinity, having K_d value in the range of 40–60 nM (Bullock *et al.*, 2005). Thus, it is likely that Pim-3 can phosphorylate these cell cycle regulators similarly as Pim-1. Supporting this idea, recombinant Pim-3 protein can phosphorylate p21/Waf *in vitro* (Morishita *et al.*, 2008). This may account for the observations that cell cycle progression was accelerated in Pim-3 transgenic mouse-derived hepatocytes compared with WT mice, as evidenced by increased proportion of the cells in G2/M phase and reciprocally decreased proportion of the cells in G0/G1 phase.

The hepatocarcinogen, DEN, induced TNF-α production consistently with the previous report (Sakurai *et al.*, 2006) and the production was further augmented by Pim-3 overexpression in liver. The crucial involvement of TNF-α in hepatocyte proliferation was proposed by the observation that liver regeneration after partial hepatectomy was impaired in mice deficient in *TNF* receptor gene (Yamada *et al.*, 1997). Moreover, accumulating evidence indicates the potential contribution of TNF-α to hepatocarcinogenesis (Roberts and Kimber, 1999; Schwabe and Brenner, 2006). Furthermore, TNF-α can promote angiogenesis, an essential process for tumorigenesis, by inducing the production of angiogenic factors, such as vascular endothelial growth factor and hepatocyte growth factor (Tamura *et al.*, 1993; Yoshida *et al.*, 1997). The production of TNF-α was regulated at several steps and the first one was at the transcription level, governed by transcription factors, such as NF-κB and Activator protein-1AP-1 (Manna *et al.*, 2000; Udalova and Kwiatkowski, 2001; Chung *et al.*, 2007). As Pim-1 can enhance NF-κB transcriptional activity (Zemskova *et al.*, 2008), Pim-3 might be able to similarly activate NF-κB, thereby inducing TNF-α expression.

It is most likely that our transgenic mice expressed a high level of the *Pim-3* transgene selectively in hepatocytes. A strong similarity of Pim-3 with another Pim kinase, Pim-1, suggests that Pim-3 can phosphorylate several cell cycle regulators and accelerate cell cycle progression as Pim-1 does. In support of this idea, we observed enhanced cell cycle progression in untreated

Pim-3 transgenic mouse-derived hepatocytes compared with that observed for WT mice. However, as evidenced by the absence of spontaneous HCC development in Pim-3 transgenic mice, accelerated hepatocyte proliferation alone cannot induce HCC. The hepatocarcinogen, DEN, can generate O^6-methlguanine and can frequently induce G-C-to-A-T transition mutations in hepatocytes (Nakatsuru *et al.*, 1993). The *Pim-3* transgene can enhance the proliferation of hepatocytes through G-C-to-A-T transition mutations, thereby accelerating HCC development. We previously observed that Pim-3 expression was detected in pre-malignant and malignant lesions but not in normal tissues of liver in humans and mice (Fujii *et al.*, 2005). Thus, Pim-3 may be a promoter but not an initiator of HCC development, and blocking of Pim-3 activity can delay and/or prevent HCC development.

Materials and methods

Preparation of Pim-3 transgenic mice

The mouse albumin enhancer/promoter region (Figure 1a) was a kind gift from Dr Palmiter (University of Washington, Seattle, WA, USA; Pinkert *et al.*, 1987). Full-length human *Pim-3* cDNA was subcloned 3 to this albumin enhancer/promoter gene. After being linearized by digestion with *Not*I, the gene was introduced into fertilized oocytes of C57BL/6 mice using a standard transgenic technique. Genomic DNA was isolated from the tail of the founder and offspring using Nucleospin tissue kit (Macherey Nagel, Düren, Germany) and genotyping was performed by PCR using a specific pair of primers, including a sense primer (5′-TTGAACTCATCGACC TGCAGGCAT-3′) flanking the upstream albumin promoter and an antisense primer (5′-GCCTTCTCGAAGCTCTCCTT GTCC-3′) inside the human *Pim-3* cDNA. Transgenic founder animals were mated with C57BL/6 mice (Charles River Japan, Yokohama, Japan). The male offspring with a heterozygous transgene were used as a transgenic group, whereas those without a transgene were used as a littermate control. All mice were kept under the specific pathogen-free conditions, and all animal experiments in this study complied with the Guidelines of the Care and Use of Laboratory Animals of Kanazawa University.

Hepatocyte isolation

Mouse hepatocytes were isolated by using a two-step perfusion method with some modifications. Briefly, under anesthetization with Avertin (2,2,2-tribromoethanol; Sigma-Aldrich, St Louis, MO, USA), a needle was inserted along the inferior vena cava and the liver was perfused sequentially with phosphate-buffered saline and collagenase-containing buffer at a rate of 5–10 ml/min. The liver was then dissected, suspended in ice-cold phosphate-buffered saline and filtered through a cell strainer with a pore size of 100 μm to remove connective tissue debris and cell clumps. After the cell suspensions were left on ice for 15 min, the resultant precipitates were collected, suspended in DMEM medium (Sigma-Aldrich) and centrifuged at 800 r.p.m. for 2 min. Cell suspensions were further centrifuged in 45% Percoll solution (Sigma-Aldrich) at 1000 r.p.m. for 10 min. The obtained cells were confirmed to consist of more than 95% hepatocytes on the basis of morphological criteria, with a viability of higher than 90% on trypan blue exclusion test. Purified hepatocytes were used for the following DNA content analysis and immunoblotting analysis.

Cell cycle analysis

The obtained hepatocytes were fixed with 70% ethanol at −20 °C. The fixed cells were incubated with 50 μg/ml propidium iodine (Molecular Probes, Eugene, OR, USA) and 1 μg/ml RNase A for 30 min at room temperature. The DNA content was then analyzed on a FACS Calibur system (BD Biosciences, Bedford, MA, USA). The distribution of cells in each cell-cycle phase was determined by cell ModFit LT software (BD Biosciences).

Protein extraction and western blotting

Hepatocytes or liver tissues were obtained and homogenized with RIPA buffer (Santa Cruz Biotechnology, Santa Cruz, CA, USA) containing proteinase inhibitor cocktail (Roche Diagnostics AG, Rotkreutz, Switzerland). After sonication for 1 min, homogenates were centrifuged at 15 000 *g* for 15 min at 4 °C to obtain the supernatants. After total protein concentrations were measured using a BCA kit (Pierce Biotechnology, Rockford, IL, USA), resultant supernatants were subjected to immunoblotting using anti-phospho-Ser^{112}-Bad, anti-phospho-Ser^{136}-Bad, anti-Bad, anti-Pim-3, anti-β actin (Sigma-Aldrich); anti-cyclin D1 (Cell Signaling Technology, Beverly, MA, USA) and anti-PCNA antibodies (BD Biosciences) as previously described (Li *et al.*, 2006).

Chemical-induced liver injury and subsequent hepatocarcinogenesis

Three-week old weaning mice were given a single intraperitoneal injection of DEN (Sigma-Aldrich), dissolved in physiological saline solution at a dose 10 mg/kg body weight as previously described (Yang *et al.*, 2006), to induce hepatocarcinogenesis. To induce acute liver injury, mice were given a dose of 100 mg/kg body weight. Serum alanine amino transferase levels were determined using a Fuji DRICHEM 55500V (Fuji Medical System, Tokyo, Japan) according to the manufacturer's instructions. Mice were killed at the indicated time intervals after the injection to conduct histopathological analysis.

RNA isolation and RT–PCR

Total RNAs were extracted from the organs using RNeasy mini kit (Qiagen, Hilden, Germany) according to the manufacturer's instructions and were further treated with RNase-free DNase (Promega, Madison, WI, USA) to deplete residual contaminated DNA. A total of 2 μg RNA was reverse-transcribed at 42 °C for 1 h in 20-μl reaction mixture containing Moloney murine leukemia virus reverse trancriptase (Toyobo, Osaka, Japan) and hexanucleotide random primer (Qiagen) to obtain cDNA as previously described (Wu *et al.*, 2008). Serially twofold diluted cDNA products were amplified for glyceraldehyde-3-phosphate dehydrogenase (GAPDH) using a specific set of primers (Table 1) using 25 cycles consisting of following reaction conditions: 94 °C for 30 s, 58 °C for 30 s and 72 °C for 1 min in a 25-μl of reaction mixture containing Taq polymerase (Takara Bio, Kyoto, Japan) to evaluate the quantity of the transcribed cDNA. Equal quantities of cDNA products were then amplified for the indicated genes using the specific sets of primers (Table 1) with 35 cycles consisting of following conditions: 94 °C for 30 s, 58 °C for 1 min and 72 °C for 1 min. The resultant PCR products were fractionated on 1.5% agarose gel and visualized by ethidium bromide staining under ultraviolet light trans-

Table 1 Sequences of the primers used for RT–PCR

Gene Name	*Forward*	*Reverse*	*Cycles*	*Length (bp)*
Mouse Pim-3	5′-GAGAGGGTCTCCCCAGAGT-3′	5′-TGGTGGCACGCTTAGGTTG-3′	35	660
Human Pim-3	5′-CGGAGGAGGGTCTCTCCAGAGTG-3′	5′-ACCCTGCGCCGGCGGAAAG-3′	35	535
Mouse TNF-α	5′-AGTTCTATGGCCCAGACCCT-3′	5′-CGGACTCCGCAAAGTCTAAG-3′	35	463
Mouse IL-1α	5′-CTCTAGAGCTCCATGCTACAGAC-3′	5′-TGGAATCCAGGGGAA ACACTG-3′	35	309
Mouse IL-1β	5′-ATGGCAACTGTTCCTGAACTCAAC T-3′	5′-CAGGACAGGTATAGATTCTTTCCTTTT-3′	35	377
GADPH	5′-ACCACAGTCCATGCCATCAC-3′	5′-TCCACCACCCTGTTGCTGTA-3′	25	431

Abbreviations: GADPH, glyceraldehydes-3-phosphate dehydrogenase; IL, interleukin; TNF, tumor necrosis factor.

illumination. The band intensities were measured using National Institutes of Health Image analysis software, version 1.62, and the ratios to GAPDH were calculated on the assumption that the ratios of untreated animals were set at 1.0.

Histopathological analysis

The liver tissue was fixed in 10% formalin buffered with phosphate-buffered saline (pH 7.2). and embedded in paraffin. Five-μm thick sections were stained with hematoxylin and eosin solution or subjected to the terminal transferase dUTP nick end labeling assay (MBL, Nagoya, Japan) according to the manufacturer's instructions. Immunohistochemical analysis was performed using anti-PNCA (BD Biosciences) or anti-cleaved caspase-3 antibodies (Cell Signaling Technology). A portion of the liver tissue was snap-frozen, dried at room temperature until the tissues firmly adhered to the slides, and was fixed in cold acetone for 10 min. The sections were blocked with serum-free Protein Block (Dako Cytomation, Glostrup, Denmark) and were incubated with rabbit anti-cyclin B1 antibodies (Santa Cruz Biotechnology). They were further incubated with Alexa Fluor 488-labeled donkey anti-rabbit IgG followed by counterstaining with 4-6-diamidino-2-phenylindole (Vector Laboratories, Burlingame, CA, USA) in dark. Immunoflurescence was visualized on a Laser Microscope 510 (Carl Zeiss, Hamburg, Germany) and cyclin B1-positive cell proportion was determined on 10 randomly chosen fields at $\times 200$ magnification. Another slides were used for staining with oil red (Sigma-Aldrich) and hematoxylin counterstaining, or immunohistochemical analysis using anti-CD31 antibodies (BD Pharmingen). The immune complexes were visualized by Envision+ System (Dako Cytomation), a catalyzed signal amplification system or the Elite ABC kit and DAB substrate kit (Vector Laboratories) according to the manufacturer's instructions. The positive cell numbers were enumerated on 10 randomly chosen visual fields at $\times 400$ magnification. The CD31-postive areas were determined as previously described (Wu *et al.*, 2008). In brief, CD31-positive areas in the tumor tissue were defined as the intratumoral vascular areas. Areas of active neovascularization (hot spot) were found inside tumor foci by scanning the section at lower magnification and the pixel numbers of CD31-positive areas were then determined on five randomly chosen fields in hot spots of each animal at $\times 400$ magnification with the help of Photoshop version 7.0. The density of neovascularization was expressed as a percentage of the whole tumor area. All histopathological examinations were conducted by an examiner without any prior knowledge of the experimental procedures. All histopathological examinations were conducted blind, by an examiner without any prior knowledge of the experimental procedures.

Statistical analysis

All obtained data were calculated and expressed as mean ± s.d. The differences were analyzed statistically using one-way analysis of variance, followed by the Turkey–Kramer test. $P<0.05$ was considered statistically significant.

Conflict of interest

The authors declare no conflict of interest.

References

Bachmann M, Hennemann H, Xing PX, Hoffmann I, Moroy T. (2004). The oncogenic serine/threonine kinase Pim-1 phosphorylates and inhibits the activity of Cdc25C-associated kinase (C-TAK-1): a novel role for Pim-1 at the G2/M cell cycle checkpoint. *J Biol Chem* **279**: 48319–48328.

Braun L, Mikumo R, Fausto N. (1989). Production of hepatocellular carcinoma by oval cells: cell cycle expression of c-myc and p53 at different stages of oval cell transformation. *Cancer Res* **49**: 1554–1561.

Bullock AN, Debreczeni J, Amos AL, Knapp S, Turk BE. (2005). Structure and substrate specificity of the Pim-1 kinase. *J Biol Chem* **280**: 41675–41682.

Chen L, Willis SN, Wei A, Smith BJ, Fletcher JI, Hinds MG *et al.* (2005). Differential targeting of prosurvival Bcl-2 proteins by their BH3-only ligands allows complementary apoptotic function. *Mol Cell* **17**: 393–403.

Chung J, Koyama T, Ohsawa M, Shibamiya A, Hoshi A, Hirosawa S. (2007). 1,25(OH)(2)D(3) blocks TNF-induced monocytic tissue factor expression by inhibition of transcription factors AP-1 and NF-kappaB. *Lab Invest* **87**: 540–547.

Deneen B, Welford SM, Ho T, Hernandez F, Kurland I, Denny CT. (2003). PIM3 proto-oncogene kinase is a common transcriptional target of divergent EWS/ETS oncoproteins. *Mol Cell Biol* **23**: 3897–3908.

Farazi PA, DePinho RA. (2006). Hepatocellular carcinoma pathogenesis: from genes to environment. *Nat Rev Cancer* **6**: 674–687.

Feldman JD, Vician L, Crispino M, Tocco G, Marcheselli VL, Bazan NG *et al.* (1998). KID-1, a protein kinase induced by depolarization in brain. *J Biol Chem* **273**: 16535–16543.

Fujii C, Nakamoto Y, Lu P, Tsuneyama K, Popivanova BK, Kaneko S *et al.* (2005). Aberrant expression of serine/threonine kinase Pim-3 in hepatocellular carcinoma development and its role in the proliferation of human hepatoma cell lines. *Int J Cancer* **114**: 209–218.

Hammerman PS, Fox CJ, Cinalli RM, Xu A, Wagner JD, Lindsten T *et al.* (2004). Lymphocyte transformation by Pim-2 is dependent on nuclear κB activation. *Cancer Res* **64**: 8341–8348.

Hosono S, Chou MJ, Lee CS, Shih C. (1993). Infrequent mutation of *p53* gene in hepatitis B virus positive primary hepatocellular carcinomas. *Oncogene* **8**: 491–496.

Kamata H, Honda S, Maeda S, Chang L, Hirata H, Karin M. (2005). Reactive oxygen species promote TNFalpha-induced death and sustained JNK activation by inhibiting MAP kinase phosphatases. *Cell* **120**: 649–661.

Li YY, Popivanova BK, Nagai Y, Ishikura H, Fujii C, Mukaida N. (2006). Pim-3, a proto-oncogene with serine/threonine kinase activity, is aberrantly expressed in human pancreatic cancer and phosphorylates bad to block bad-mediated apoptosis in human pancreatic cancer cell lines. *Cancer Res* **66**: 6741–6747.

Ma W, Xia X, Stafford LJ, Yu C, Wang F, LeSage G *et al.* (2006). Expression of GCIP in transgenic mice decreases susceptibility to chemical hepatocarcinogenesis. *Oncogene* **25**: 4207–4216.

Maeda S, Kamata H, Luo JL, Leffert H, Karin M. (2005). IKKbeta couples hepatocyte death to cytokine-driven compensatory proliferation that promotes chemical hepatocarcinogenesis. *Cell* **121**: 977–990.

Manna SK, Mukhopadhyay A, Aggarwal BB. (2000). Leflunomide suppresses TNF-induced cellular responses: effects on NF-kappa B, activator protein-1, c-Jun N-terminal protein kinase, and apoptosis. *J Immunol* **165**: 5962–5969.

Mochizuki T, Kitanaka C, Noguchi K, Muramatsu T, Asai A, Kuchino Y. (1999). Physical and functional interactions between Pim-1 kinase and Cdc25A phosphatase. Implications for the Pim-1-mediated activation of the c-Myc signaling pathway. *J Biol Chem* **274**: 18659–18666.

Morishita D, Katayama R, Sekimizu K, Tsuruo T, Fujita N. (2008). Pim kinases promote cell cycle progression by phosphorylating and down-regulating p27Kip1 at the transcriptional and posttranscriptional levels. *Cancer Res* **68**: 5076–5085.

Nakatsuru Y, Matsukuma S, Nemoto N, Sugano H, Sekiguchi M, Ishikawa T. (1993). O^6-methylguanine-DNA methyltransgerase protects against nitrosamine-induced hepatocarcinogenesis. *Proc Natl Acad Sci USA* **90**: 6468–6472.

Otani K, Korenaga M, Beard MR, Li K, Qian T, Showalter LA *et al.* (2005). Hepatitis C virus core protein, cytochrome P450 2E1, and alcohol produce combined mitochondrial injury and cytotoxicity in hepatoma cells. *Gastroenterology* **128**: 96–107.

Pinkert CA, Ornitz DM, Brinster RL, Palmiter RD. (1987). An albumin enhancer located 10 kb upstream functions along with its promoter to direct efficient, liver-specific expression in transgenic mice. *Genes Dev* **1**: 268–276.

Popivanova BK, Li YY, Zheng H, Omura K, Fujii C, Tsuneyama K *et al.* (2007). Proto-oncogene, Pim-3 with serine/threonine kinase activity, is aberrantly expressed in human colon cancer cells and can prevent Bad-mediated apoptosis. *Cancer Sci* **98**: 321–328.

Qian KC, Wang L, Hickey ER, Studts J, Barringer K, Peng C *et al.* (2005). Structural basis of constitutive activity and a unique nucleotide binding mode of human Pim-1 kinase. *J Biol Chem* **280**: 6130–6137.

Roberts RA, Kimber I. (1999). Cytokines in genotoxic hepatocarcinogenesis. *Carcinogenesis* **20**: 1297–1401.

Sakurai T, Maeda S, Chang L, Karin M. (2006). Loss of hepatic NF-kappa B activity enhances chemical hepatocarcinogenesis through sustained c-Jun N-terminal kinase 1 activation. *Proc Natl Acad Sci USA* **103**: 10544–10551.

Schwabe RF, Brenner DA. (2006). Mechanisms of liver injury. I. TNF-alpha-induced liver injury: role of IKK, JNK, and ROS pathways. *Am J Physiol Gastrointest Liver Physiol* **290**: G583–G589.

She QB, Solit DB, Ye Q, O'Reilly KE, Lobo J, Rosen N. (2005). The BAD protein integrates survival signaling by EGFR/MAPK and PI3K/Akt kinase pathways in PTEN-deficient tumor cells. *Cancer Cell* **8**: 287–297.

Tamura M, Arakaki N, Tsuboushi H, Takada H, Daikuhara Y. (1993). Enhancement of human hepatocyte growth factor production by interleukin-1α and -1β and tumor necrosis factor-α by fibroblasts in culture. *J Biol Chem* **268**: 8140–8145.

Thorgeirsson SS, Grisham JW. (2002). Molecular pathogenesis of human hepatocellular carcinoma. *Nat Genet* **31**: 339–346.

Udalova IA, Kwiatkowski D. (2001). Interaction of AP-1 with a cluster of NF-kappa B binding elements in the human TNF promoter region. *Biochem Biophys Res Commun* **289**: 25–33.

Umemura T, Ichijo T, Yoshizawa K, Tanaka E, Kiyosawa K. (2009). Epidemiology of hepatocellular carcinoma in Japan. *J Gastroenterol* **44**(Suppl 19): 102–107.

Verna L, Whysner J, Williams GM. (1996). N-nitrosodiethylamine mechanistic data and risk assessment: bioactivation, DNA-adduct formation, mutagenicity, and tumor initiation. *Pharmacol Ther* **71**: 57–81.

Wang Y, Ausman LM, Geenberg AS, Russel RM, Wang X-D. (2009). Nonalcoholic steatohepatitis induced by a high-fat diet promotes diethylnitrosamine-initiated early hepatocarcinogenesis in rats. *In t J Cancer* **124**: 540–546.

Wang Z, Bhattacharya N, Mixter PF, Wei W, Sedivy J, Magnuson NS. (2002). Phosphorylation of the cell cycle inhibitor p21Cip1/WAF1 by Pim-1 kinase. *Biochim Biophys Acta* **1593**: 45–55.

Wu Y, Li YY, Matsushima K, Baba T, Mukaida N. (2008). CCL3–CCR5 axis regulates intratumoral accumulation of leukocytes and fibroblasts and promotes angiogenesis in murine lung metastasis process. *J Immunol* **181**: 6384–6393.

Yamada Y, Kirillova I, Peschon JJ, Fausto N. (1997). Initiation of liver growth by tumor necrosis factor: deficient liver regeneration in mice lacking type I tumor necrosis factor receptor. *Proc Natl Acad Sci USA* **94**: 1441–1446.

Yang E, Zha J, Jockel J, Boise LH, Thompson CB, Korsmeyer SJ. (1995). Bad, a heterodimeric partner for Bcl-XL and Bcl-2, displaces Bax and promotes cell death. *Cell* **80**: 285–291.

Yang X, Lu P, Fujii C, Nakamoto Y, Gao JL, Kaneko S *et al.* (2006). Essential contribution of a chemokine, CCL3, and its receptor, CCR1, to hepatocellular carcinoma progression. *Int J Cancer* **118**: 1869–1876.

Yoshida S, Ono M, Shono T, Izumi H, Ishibashi T, Suzuki H *et al.* (1997). Involvement of interleukin-8, vascular endothelial growth factor, and basic fibroblast growth factor in tumor necrosis factor α-dependent angiogenesis. *Mol Cell Biol* **17**: 4015–4023.

Zemskova M, Sahakian E, Bashkirova S, Lilly M. (2008). The PIM1 kinase is a critical component of a survival pathway activated by docetaxel and promotes survival of docetaxel-treated prostate cancer cells. *J Biol Chem* **283**: 20635–20644.

Zha J, Harada H, Yang E, Jockel J, Korsmeyer SJ. (1996). Serine phosphorylation of death agonist BAD in response to survival factor results in binding to 14-3-3 not BCL-X(L). *Cell* **87**: 619–628.

Zheng HC, Tsuneyama K, Takahashi H, Miwa S, Sugiyama T, Popivanova BK *et al.* (2008). Aberrant Pim-3 expression is involved in gastric adenoma-adenocarcinoma sequence and cancer progression. *J Cancer Res Clin Oncol* **134**: 481–488.

Zheng Y, Chen WL, Louie SG, Yen TS, Ou JH. (2007). Hepatitis B virus promotes hepatocarcinogenesis in transgenic mice. *Hepatology* **45**: 16–21.